J|A|C|S COMMUNICATIONS

Published on Web 09/22/2009

Electronic Coulombic Coupling of Excitation-Energy Transfer in Xanthorhodopsin

Kazuhiro J. Fujimoto and Shigehiko Hayashi*

Department of Chemistry, Graduate School of Science, Kyoto University, Kyoto 606-8520, Japan

Received July 10, 2009; E-mail: hayashig@kuchem.kyoto-u.ac.jp

Excitation-energy transfer (EET)[1] is a well-known phenomenon observed in pairs or aggregates of molecules, and its feature is widely used in biological systems such as green-plant photosynthesis.[2] Recently, a new biological EET system was found in xanthorhodopsin (xR),[3] which is a retinal protein[4] and includes not only a common chromophore, retinal (RET), but also a light harvesting carotenoid antenna, salinixanthin (SXN) (Figure 1). Differing from the conventionally found photosynthetic systems, the components relevant to EET are only SXN and RET with a 1:1 ratio. Therefore, the antenna system, quite smaller and simpler than photosynthetic systems, is expected to be a fundamental model for thorough understanding of the EET mechanism. To physically characterize EET in xR, several experimental studies have been carried out,[5] while theoretical study has not been performed yet due to a lack of structural information. However, an X-ray crystallographic structure was solved in 2008,[6] which opens the door toward theoretical investigations.

The EET efficiency depends on the electronic coupling between donor and acceptor molecules which is often called the pseudo-Coulombic interaction (PCI).[1] To compute it, the dipole−dipole (dd) approximation, which is derived from the leading term of the multipole expansion of the electronic coupling, is frequently used because of its simplicity,

$$V_{Coul} = \langle \Psi_e^D \cdot \Psi_g^A | V | \Psi_g^D \cdot \Psi_e^A \rangle \approx [\hat{\mathbf{r}}_D \cdot \hat{\mathbf{r}}_A - 3(\hat{\mathbf{r}}_D \cdot \hat{\mathbf{e}}_R)(\hat{\mathbf{r}}_A \cdot \hat{\mathbf{e}}_R)]/4\pi\varepsilon_0 R^3 \equiv V_{Coul}^{dd} \quad (1)$$

where $\hat{\mathbf{r}}_X$ denotes the transition dipole moment of the molecule X (D: donor and A: acceptor), and R and $\hat{\mathbf{e}}_R$ are the distance between centers of the D and A molecules and its unit vector, respectively. As seen in eq 1, PCI depends sensitively on alignment of the D and A molecules, especially mutual orientations. To accurately calculate PCI, however, the dd approximation is limited for $D-A$ molecules that are largely separated compared with their molecular sizes.[1b] Considering a smaller distance between RET and SXN (∼13 Å) than their molecular sizes (∼36 Å), eq 1 would be out of range for EET in xR. A practical difficulty in this regard arises in defining of the molecular centers at which the transition dipole moments are placed since V_{Coul}^{dd} strongly depends on the definitions in this case. To overcome this problem, we developed the transition-density-fragment interaction (TDFI) method. Assuming negligible overlap between electronic wave functions (WFs) of the initial and final states, the interactions were represented using transition densities (TrDs) as follows,

$$V_{Coul}^{TDFI} = \int d\mathbf{r}_1 \int d\mathbf{r}_2 \rho_{ge}^A(\mathbf{r}_1)\rho_{ge}^D(\mathbf{r}_2)/r_{12} = \sum_{\mu,\nu\in A} P_{\nu\mu}^A \sum_{\lambda,\sigma\in D} P_{\lambda\sigma}^D(\mu\nu|\sigma\lambda) = \sum_{\mu,\nu\in A} P_{\nu\mu}^A V_{\mu\nu}^D \quad (2)$$

where $P_{\lambda\sigma}^X$ denotes the TrD matrix between the ground and excited states for the D and A molecules, and $(\mu\nu|\sigma\lambda)$ indicates a two-electron integral in an atomic orbital (AO) representation. For computing the donor potential $V_{\mu\nu}^D$ in eq 2, the DFI algorithm[7] was used (see Supporting Information (SI) for details). The TDFI method is based on the AO integrals and the self-consistent TrDs, which can describe PCI more accurately than the previously proposed method[1b] (see SI). It is noteworthy that the TDFI method is free from the aforementioned molecular center problem.

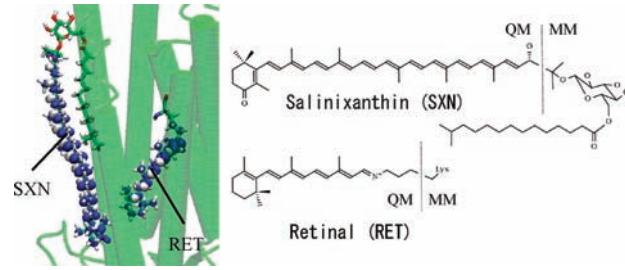

Figure 1. QM/MM optimized structures of SXN and RET in xR. Transition density distributions are also shown.

To obtain the TrDs, we adopted the symmetry-adapted cluster-CI (SAC-CI)[8] method for RET and time-dependent (TD) density-functional theory (DFT)[9] with B3LYP[10] and the revised Coulomb-attenuating method (rCAM-)[11] B3LYP functionals for SXN. As shown in our previous paper, SAC-CI accurately describes the excited states of retinal proteins.[12] The crystallographic structure[6] was refined via two steps. First, a 5 ns molecular dynamics (MD) simulation was carried out for a periodic boundary box (90 × 90 × 120 Å^3) composed of the xR protein and a 1-Palmitoyl-2-Oleoyl-Phosphatidyl Ethanolamine (POPE) membrane, using a time step of 2 fs under NPT conditions at 300 K and 1 atm (see SI). The geometry was then optimized with an *ab initio* quantum mechanical/molecular mechanical (QM/MM) method[7,13] at the rCAM-B3LYP/Amber99[14] level of theory. The split valence double-ζ plus polarization basis set (6-31G(d)) was used for all QM atoms. The $C_\beta-C_\gamma$ bond of lysine-240 and the $C_{1'}-C_{2'}$ bond of SXN were cut as the QM/MM boundary, and those were capped with hydrogen. A negligibly small overlap between WFs of the initial and final states (∼10^{-10}) was found (see SI), confirming the validity of TDFI method. The QM/MM computations were carried out with TINKER4.2[15] interfaced with Gaussian03.[16] The TDFI program was implemented in Gaussian03. All MD calculations were performed with AMBER9.[17]

Table 1 summarizes V_{Coul}^{TDFI} and compares them with the experimental values[18] and V_{Coul}^{dd}. The TDFI values obtained with TD-rCAM-B3LYP/SAC-CI (216.2 cm^{-1}) and TD-B3LYP/SAC-CI (222.8 cm^{-1}) nicely agree with the experimental one (160−210 cm^{-1})[18] and are successfully improved compared with V_{Coul}^{dd} (732.6 and 751.0 cm^{-1}) by more than 500 cm^{-1}. The excitation energies calculated with TD-B3LYP/SAC-CI (2.41 eV for SXN and 2.05 eV for RET) also reproduce well the experimental values[3] (2.55 eV for SXN and 2.21 eV for RET) (see SI). It is noted that other

10.1021/ja905697n CCC: $40.75

Table 1. Absolute Pseudo-Coulombic Interactions (cm^{-1})

method	TD-B3LYP/SAC-CI	TD-rCAM-B3LYP/SAC-CI	expt[a]
TDFI	222.8 (233.3)[b]	216.2 (231.1)[b]	160−210
dd	751.0 (755.5)[b]	732.6 (752.0)[b]	
TCI	224.5	217.9	

[a] Reference 18. [b] Without protein.

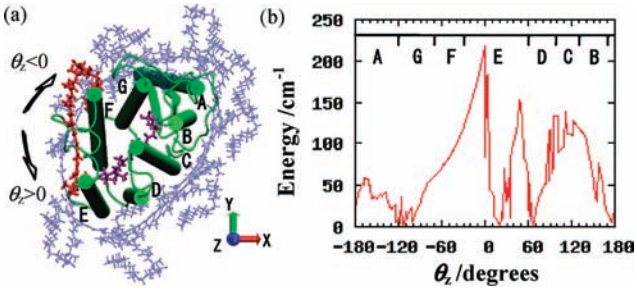

Figure 2. (a) Top view of the SXN conformations virtually generated along θ_z. Only 12 conformations are shown in blue. (b) Theoretical PCI curve obtained with the TrESP method.

WFs (TD-B3LYP, TD-rCAM-B3LYP, and CI for all Singles) for RET overestimated PCI by more than 120 cm^{-1} (see SI), indicating that an accurate method is required to describe the complex nature of WFs of RET. It was also found that V_{Coul}^{TDFI} is insensitive to the DFT functional used for SXN and to the protein electrostatic potential (ESP) as seen in Table 1. Large errors of V_{Coul}^{dd} are due to the aforementioned problem of the dd approximation; as shown in Figure 1, the TrD spreads over each of the *D* and *A* molecules to an extent comparable with the *D*−*A* distance, and thus the dd approximation does not hold in this case.

The accurate evaluation of PCI allowed us to investigate the molecular architecture of the chromophore−protein complex that attains efficient EET. To examine the correlation between the SXN-RET alignment and the EET efficiency, we computed PCIs for SXN conformations that are virtually generated around the protein as depicted in Figure 2a. The SXN conformations on the protein surface were searched along an angle, θ_Z, which is an azimuth around the membrane normal axis lying on the protein center. At each θ_Z angle, the search is performed for the rigid body rotation of SXN combined with the radial shift (see SI). PCIs for the SXN conformations along θ_Z were then evaluated. For computation of PCIs, we adopted the transition charge from the ESP (TrESP) method.[19] In this method, PCI is represented by a classical Coulombic interaction between the 'transition' charges which are determined with TrD via the conventional ESP fitted charge scheme. The TrESP method drastically reduces the computational costs for evaluation of PCI and thus enables one to calculate PCIs for many SXN conformations. As listed in Table 1, TrESP values are in good agreement with TDFI ones.

Figure 2b shows PCIs obtained with the TrESP method for the generated SXN conformations. The largest peak (217.9 cm^{-1}) appears for the native conformation at $\theta_Z = 0$, indicating that the most efficient EET occurs in the native conformation. The second largest peak (153.3 cm^{-1}) was obtained at 48°. Using the experimental time constants of the SXN S_2 lifetime (110 fs) and of EET (165 fs)[18] and the Fermi's golden rule relation, $k_{EET} \propto V_{Coul}^2$, the EET efficiency, $k_{EET}/(k_{EET} + k_{rd})$, at 48° is evaluated to be 25%, which is significantly reduced by 15% compared with the native one (40%). The results clearly demonstrate that optimal SXN alignment for the maximally tuned efficiency of EET is attained in the native xR.

One may notice in Figure 2b a characteristic monotonic increase of PCI in the region $\theta_Z = -80°-0°$. This feature is a consequence of SXN alignment along a widely open groove on the protein surface between E and F helices (see Figure 2a). At the bottom of the groove at $\theta_Z = 0$, SXN aligns in the native conformation. Thus the widely open groove may act as a funnel that leads SXN to optimal alignment.

Among retinal proteins, archaerhodopsin-2 (aR2) is also known to bind a carotenoid, bacterioruberin.[20] In contrast to xR, however, no EET activity is found in aR2. To elucidate the origin for the distinct difference in EET activity, we also computed the PCI between the *D* and *A* molecules in the conformations observed in aR2 (see SI). The PCI was calculated to be 5.9 cm^{-1}, which is much smaller than that in xR (217.9 cm^{-1}) and thus well explains lack of EET in aR2. The considerable reduction of PCI is mainly attributed to the mismatch of the mutual orientations rather than an increase of the *D*−*A* distance since the distance increases only modestly (∼13 Å (xR) and ∼17 Å (aR2) for the center-to-center distances).

Here, we proposed the TDFI approach for EET and succeeded in an accurate evaluation of PCI observed in xR. This method makes it possible to investigate EET systems where the dd approximation breaks down and can be easily extended to other WFs. The high accuracy and the wide applicability of the methods would also enable one to analyze and design FRET (fluorescence resonance energy transfer) systems widely utilized in bioimaging.

Acknowledgment. This study was supported by a Grant-in-Aid for Young Scientists (B) from the Ministry of Education, Culture, Sports, Sciences, and Technology of Japan, and others (see SI).

Supporting Information Available: Detailed descriptions of the TDFI method, the structural information, and complete refs 16 and 17. This material is available free of charge via the Internet at http://pubs.acs.org.

References

(1) (a) Förster, T. In *Modern Quantum Chemistry*; Sinanoglu, O., Ed.; Academic Press: New York, 1965; Vol. *III*, pp 93−137. (b) Krueger, B. P.; Scholes, G. D.; Fleming, G. R. *J. Phys. Chem. B* **1998**, *102*, 5378. (c) Damjanović, A.; Ritz, T.; Schulten, K. *Phys. Rev. E* **1999**, *59*, 3293.
(2) van Grondelle, R.; Dekker, J. P.; Gillbro, T.; Sundstrom, V. *Biochim. Biophys. Acta* **1994**, *1187*, 1.
(3) Balashov, S. P.; Imasheva, E. S.; Boichenko, V. A.; Antón, J.; Wang, J. M.; Lanyi, J. K. *Science* **2005**, *309*, 2061.
(4) Mathies, R. A.; Lugtenburg, J. In *Handbook of Biological Physics*; Stavenga, D. G., Grip, W. J. d., Pugh, E. N., Eds.;Elsevier Science B. V.: Amsterdam, 2000; Vol. 3, pp 55−90.
(5) Lanyi, J. K.; Balashov, S. P. *Biochim. Biophys. Acta* **2008**, *1777*, 684.
(6) Luecke, H.; Schobert, B.; Stagno, J.; Imasheva, E. S.; Wang, J. M.; Balashov, S. P.; Lanyi, J. K. *Proc. Natl. Acad. Sci. U.S.A.* **2008**, *105*, 16561.
(7) Fujimoto, K.; Yang, W.-T. *J. Chem. Phys.* **2008**, *129*, 054102.
(8) Nakatsuji, H. *Chem. Phys. Lett.* **1978**, *59*, 362.
(9) Bauernschmitt, R.; Ahlrichs, R. *Chem. Phys. Lett.* **1996**, *256*, 454.
(10) Lee, C.; Yang, W.-T.; Parr, R. G. *Phys. Rev. B* **1988**, *37*, 785.
(11) Cohen, A. J.; Mori-Sánchez, P.; Yang, W.-T. *J. Chem. Phys.* **2007**, *126*, 191109.
(12) (a) Fujimoto, K.; Hayasji, S.; Hasegawa, J.; Nakatsuji, H. *J. Chem. Theory Comput.* **2007**, *3*, 605. (b) Fujimoto, K.; Hasegawa, J.; Nakatsuji, H. *Chem. Phys. Lett.* **2008**, *462*, 318.
(13) Warshel, A.; Levitt, M. *J. Mol. Biol.* **1976**, *103*, 227.
(14) Wang, J.; Cieplak, P.; Kollman, P. A. *J. Comput. Chem.* **2000**, *21*, 1049.
(15) Ponder, J. W. *Tinker4.2*; Washington University: St. Louis, MO, 2004.
(16) Frisch, M. J., et al. *Gaussian03*; Gaussian, Inc.: Pittsburgh, PA, 2003.
(17) Case, D. A., et al. *AMBER 9*; University of California: San Francisco, CA, 2006.
(18) Polívka, T.; Balashov, S. P.; Chábera, P.; Imasheva, E. S.; Yartsev, A.; Sundström, V.; Lanyi, J. K. *Biophys. J.* **2009**, *96*, 2268.
(19) Madjet, M. E.; Abdurahman, A.; Renger, T. *J. Phys. Chem. B* **2006**, *110*, 17268.
(20) Yoshimura, K.; Kouyama, T. *J. Mol. Biol.* **2008**, *375*, 1267.

JA905697N